Orbital rendezvous performance comparison of differential geometric and ZEM/ZEV feedback guidance algorithms

Pengyu Wang[1], Yanning Guo[1], and Bong Wie[2] (✉)

1. Department of Control Science and Engineering, Harbin Institute of Technology, Harbin 150001, China
2. Department of Aerospace Engineering, Iowa State University, Ames, IA 50011, USA

ABSTRACT

In this paper, the performance of two distinct classes of feedback guidance algorithms is evaluated for a spacecraft rendezvous problem utilizing a continuous low-thrust propulsion system. They are the DG (Differential Geometric) and ZEM/ZEV (Zero-Effort-Miss/Zero-Effort-Velocity) feedback guidance algorithms. Even though these two guidance algorithms do not attempt to minimize the onboard fuel consumption or ΔV directly, the ΔV requirement is used as a measure of their orbital rendezvous performance for various initial conditions and a wide range of the rendezvous time (within less than one orbital period of the target vehicle). For the DG guidance, the effects of its guidance parameter and terminal time on the closed-loop performance are evaluated by numerical simulations. For the ZEM/ZEV guidance, its near-fuel-optimality is further demonstrated for a rapid, short-range orbital rendezvous, in comparison with the corresponding open-loop optimal solutions. Furthermore, the poor ΔV performance of the ZEM/ZEV guidance for a slow, long-range orbital rendezvous is remedied by simply adding an initial drift phase. The ZEM/ZEV feedback guidance algorithm and its appropriate variants are then shown to be a simple practical solution to a non-impulsive rendezvous problem, in comparison with the DG guidance as well as the open-loop optimal guidance.

1   Introduction

On-orbit satellite servicing missions, currently being envisioned by commercial space industry, DARPA (Defense Advanced Research Projects Agency), and NASA, will certainly require fuel-optimal, autonomous rendezvous and proximity operations. A variety of techniques for rendezvous and proximity operations have been developed and successfully flight demonstrated for various space missions in the past few decades. They include the classical methods, such as V-bar, R-bar, and glideslope hopping approaches, which basically employ multiple impulsive ΔV maneuvers for rendezvous and proximity operations [1–4]. However, such flight-proven, classical multi-impulse approaches may not be directly applicable to future on-orbit servicing missions, such as refuelling geosynchronous (GEO) satellites [5] and removing space debris [6, 7], that employ servicing spacecraft equipped with continuous low-thrust electric propulsion systems.

In the past two decades, a considerable amount of research effort has also been devoted to developing a variety of optimal autonomous orbital rendezvous techniques. The DG (Differential Geometric) guidance and the ZEM/ZEV (Zero-Effort-Miss/Zero-Effort-Velocity) guidance are two distinct classes of feedback guidance approaches. The continuous (non-impulsive) feedback control nature of these two approaches makes them more suitable to deal with various uncertainties and perturbations.

The trajectories of space vehicles can be characterized as space curves. Classical differential geometry theory characterizes space curves in terms of the curvature and torsion parameters, resulting in a somewhat mathematical approach to design a guidance algorithm. On account of this, a class of feedback guidance relying

✉ bongwie@iastate.edu

on the Frenet–Serret formula of classical differential geometry theory has been developed in the past few decades. The DG guidance algorithm was first presented in Ref. [8] for a three-dimensional missile interception to guarantee the capture of a maneuvering target, which has some advantages of robustness and low control thrust. The acceleration of the DG guidance algorithm was then transformed from the arc-length system to the time domain, and the target capturability was investigated under various initial conditions in Refs. [9–12]. The two-dimensional DG guidance algorithm was developed as well without using the torsion parameter, and improved by fuzzy PID and gain-varying techniques in Refs. [13–15]. In fact, the DG guidance algorithm shares the same spirit with the classical proportional navigation (PN) guidance approach or its variants [16]. Drawing lessons from the PN guidance, a simple and explicit three-dimensional DG guidance algorithm was designed and its guidance performance was qualitatively analyzed by a Lyapunov-like approach in Refs. [17–20]. Apart from the above researches, some distinct guidance algorithms also have been proposed for missile interception using the differential geometry concepts in Refs. [21, 22]. Recently, a two-dimensional spacecraft rendezvous DG guidance algorithm is proposed in Ref. [23], which requires proper selection of three design parameters: the navigation ratio and the two velocity control gains. In this paper, expanding upon the research results described in Ref. [23], we will further examine the DG rendezvous guidance algorithm in comparison with the ZEM/ZEV guidance as well as the corresponding open-loop optimal solutions.

The ZEM/ZEV feedback guidance algorithm is based on an optimal control formulation of minimizing the total control energy, given the terminal-time value, assuming that the gravity field is either constant or an explicit function of time [24, 25]. This algorithm is conceptually simple and easy to apply, thus has great potential for autonomous onboard implementation. For many practical missions, the gravity vector is neither constant nor an explicit function of time, but is a function of the orbital position vector, which causes the non-optimality of the ZEM/ZEV guidance algorithm. However, even for such space missions, the desired acceleration of the ZEM/ZEV algorithm can still be obtained by integrating or propagating the orbital dynamics and its near-optimal performance has been observed for various illustrative applications in Refs. [26–31]. The

ZEM/ZEV guidance algorithm and its variants, such as predictive guidance and pulsed PN guidance, have been also studied for a future advanced space mission for deflecting or disrupting a hazardous asteroids in Ref. [32]. A slower orbital rendezvous (i.e., with a larger terminal time) is known to be always better in minimizing the total control energy regardless of the initial conditions. This somewhat nontrivial issue is discussed in Ref. [30] by generating the open-loop optimal solutions via general pseudo-spectral optimal control software (GPOPS) package. Unfortunately, the ZEM/ZEV guidance algorithm wrongfully indicates a local optimal-ΔV rendezvous time because the ΔV performance of ZEM/ZEV rapidly deteriorates as the rendezvous time approaches the orbital period. To improve the ZEM/ZEV guidance performance for long-range missions, a waypoint-optimized ZEM/ZEV algorithm was proposed in Refs. [27, 28], which divides the terminal time into several segments with intermediate waypoints. In Refs. [27, 28], it was shown that the waypoint-optimized ZEM/ZEV algorithm can even compete with the corresponding open-loop optimal solutions for long-range orbital transfer and Mars landing problems.

In this paper, expanding upon the previous research results as discussed above, we will compare the orbital rendezvous performance of the DG and ZEM/ZEV guidance algorithms in terms of their actual fuel consumption (characterized by ΔV) for various initial conditions and a wide range of rendezvous time (but within less than one orbital period of the target vehicle). This paper is organized as follows. The mathematical formulation of DG guidance algorithm will be briefly reviewed and further analyzed in Section 2. The optimal feedback guidance problem and the generalized ZEM/ZEV guidance algorithm will also be reviewed briefly in Section 3. Additionally, a waypoint ZEM/ZEV algorithm is developed to improve the guidance performance of a slower orbital rendezvous in this section, which provides a drift phase at the beginning of the engagement. Note that the algorithm presented here is an extension of the two-phase ZEM/ZEV concept proposed in Ref. [31] for the Mars and Lunar landing problems. The performance of the two distinct guidance algorithms will be evaluated and compared for various initial conditions and a wide range of terminal time in Section 4. The effectiveness of the new two-phase ZEM/ZEV guidance concept will also be demonstrated in Section 4, which

results in an improved ΔV performance of the ZEM/ZEV guidance algorithm, especially for a slower, non-impulsive rendezvous.

2   Differential Geometric (DG) guidance

2.1   Dynamical modeling for an orbital rendezvous

For a point-mass model of the chaser and target spacecraft, their flight trajectories can be characterized as continuous smooth curves in space. The Frenet–Serret formula of classical differential geometry theory are then used to describe the characteristics of space curves with respect to arc-length, as follows:

$$
\begin{bmatrix} \boldsymbol{t}'(s) \\ \boldsymbol{n}'(s) \\ \boldsymbol{b}'(s) \end{bmatrix} = \begin{bmatrix} 0 & \kappa(s) & 0 \\ -\kappa(s) & 0 & \tau(s) \\ 0 & -\tau(s) & 0 \end{bmatrix} \begin{bmatrix} \boldsymbol{t}(s) \\ \boldsymbol{n}(s) \\ \boldsymbol{b}(s) \end{bmatrix} \quad (1)
$$

where $\kappa(s)$ and $\tau(s)$ are respectively the curvature and torsion parameters of the curve; $\boldsymbol{t}(s)$, $\boldsymbol{n}(s)$, and $\boldsymbol{b}(s)$ are unit vectors associated with the tangential, normal, and binormal directions of the space curve, respectively; ( )' represents the derivative with respect to the arc-length s.

According to the classical differential geometry theory, the curve shape in the plane spanned by vectors $\boldsymbol{t}(s)$ and $\boldsymbol{n}(s)$ is determined by the curvature $\kappa(s)$, while in the plane spanned by vectors $\boldsymbol{t}(s)$ and $\boldsymbol{b}(s)$ it is determined by the torsion $\tau(s)$. For a two-dimensional rendezvous problem illustrated in Fig. 1, the curvature $\kappa(s)$ is considered as the control command which needs to be properly designed by ignoring the torsion.
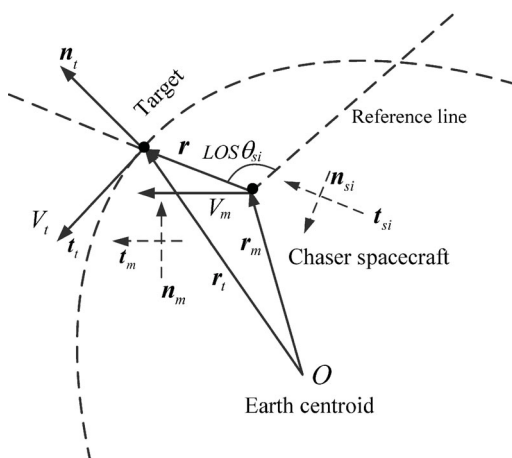

Fig. 1   Geometric description of a near-distance rendezvous problem. Reproduced from Ref. [23], ©IAA 2006.

As shown in Fig. 1, we have

$$
\boldsymbol{r}_m = \boldsymbol{r}_t - \boldsymbol{r} \quad (2)
$$

where $\boldsymbol{r}_t$ and $\boldsymbol{r}_m$ are the position vectors of the target and chaser spacecraft in the Earth-Centered Inertial (ECI) coordinate system; $\boldsymbol{r}$ is the line-of-sight (LOS) vector. In this paper, we adopt the same notations $\boldsymbol{r}_m$, $\boldsymbol{r}_t$, and $\boldsymbol{r}$ used in Ref. [23], which is often employed in the missile guidance literatures. In addition, the relative range between the chaser and target is denoted by r, that is, the magnitude of the LOS vector.

To simplify the guidance algorithm design, the target is assumed in a two-dimensional circular or near-circular orbit, which means that the target speed V_t is constant, while the speed of chaser spacecraft V_m is not constant. Defining the arc-lengths of the chaser and target flight trajectories as s_m and s_t, we have

$$
\frac{\mathrm{d}s_m}{\mathrm{d}t} = V_m, \quad \frac{\mathrm{d}s_t}{\mathrm{d}t} = V_t \quad (3)
$$

Taking the derivative of Eq. (2) with respect to s_m, we obtain the kinematical equation and its associated scalar components along the tangential and normal directions of the LOS vector, as follows:

$$
\boldsymbol{t}_m = \frac{V_t}{V_m}\boldsymbol{t}_t - r'\boldsymbol{t}_{si} - r\omega\boldsymbol{n}_{si} \quad (4)
$$

$$
r' = \frac{V_t}{V_m}\boldsymbol{t}_t \cdot \boldsymbol{t}_{si} - \boldsymbol{t}_m \cdot \boldsymbol{t}_{si} \quad (5)
$$

$$
r\omega = \frac{V_t}{V_m}\boldsymbol{t}_t \cdot \boldsymbol{n}_{si} - \boldsymbol{t}_m \cdot \boldsymbol{n}_{si} \quad (6)
$$

where subscripts m, t, and si represent the chaser, target, and LOS, respectively; ω is the LOS rotation rate in arc-length system (i.e., $\omega = \theta'_{si}$); θ_{si} denotes the LOS angle from a reference line as shown in Fig. 1. Moreover, r' can be taken as the closing speed between the chaser and target which is expressed in the arc-length system.

Taking the derivative of Eq. (4) with respect to s_m again, and applying the Frenet–Serret formula, we then obtain the following set of orbital rendezvous dynamical equations [23]:

$$
r'' - r\omega^2 = \frac{V_t^2}{V_m^2}\kappa_t(\boldsymbol{n}_t \cdot \boldsymbol{t}_{si}) - \kappa_m(\boldsymbol{n}_m \cdot \boldsymbol{t}_{si}) - \frac{V_t}{V_m^3}\frac{\mathrm{d}V_m}{\mathrm{d}t}(\boldsymbol{t}_t \cdot \boldsymbol{t}_{si}) \quad (7)
$$

$$
r\omega' + 2r'\omega = \frac{V_t^2}{V_m^2}\kappa_t(\boldsymbol{n}_t \cdot \boldsymbol{n}_{si}) - \kappa_m(\boldsymbol{n}_m \cdot \boldsymbol{n}_{si}) - \frac{V_t}{V_m^3}\frac{\mathrm{d}V_m}{\mathrm{d}t}(\boldsymbol{t}_t \cdot \boldsymbol{n}_{si}) \quad (8)
$$

2.2 DG guidance algorithm for rendezvous

As mentioned previously, the DG approach focuses on the shape of flight trajectories, which leads to a novel and direct approach for guidance algorithm design. To the best of authors' knowledge, most of the DG guidance algorithms were developed for the problem of missile interception, except for Ref. [23] which addressed the orbital rendezvous example. Different from the interception problem, the following constraints should be considered when the DG guidance is applied for the near-distance rendezvous. (1) The relative range r should decrease to zero, i.e., $r \to 0$, which guarantees the approach. (2) As the relative range decrease, the closing speed should also decrease to zero, i.e., $r' \to 0$, which is necessary condition for the rendezvous problem. (3) The LOS rotation rate should decrease.

The DG algorithm is often developed in the arc-length system with respect to s_m. However, the curvature command is not practical because the arc-length cannot be measured by onboard sensors. In order to resolve this problem, the acceleration command of the DG guidance algorithm is transformed from the arc-length system to the time domain, and was applied to the ballistic missile defense scenario in Ref. [13].

Finally, we can obtain a two-dimensional DG rendezvous algorithm according to the dynamical equations (7) and (8). The curvature command κ_m and acceleration command a_{vc} in time domain are proposed in Ref. [23], as follows:

$$\kappa_m = \frac{1}{V_m^2} \left(V_t^2 \kappa_t \frac{\boldsymbol{n}_t \cdot \boldsymbol{n}_{si}}{\boldsymbol{n}_m \cdot \boldsymbol{n}_{si}} - a_{vc} \frac{V_t}{V_m} \frac{\boldsymbol{t}_t \cdot \boldsymbol{n}_{si}}{\boldsymbol{n}_m \cdot \boldsymbol{n}_{si}} - N \frac{\dot{r}\dot{\theta}_{si}}{\boldsymbol{n}_m \cdot \boldsymbol{n}_{si}} \right) \tag{9}$$

$$a_{vc} = \frac{\mathrm{d}V_m}{\mathrm{d}t} = M_r r + M_v \dot{r} \tag{10}$$

where N is the navigation ratio; M_r and M_v are the V_m-control gains; κ_t is the curvature of the target flight trajectory; $\dot{r}$ and $\dot{\theta}$ are the expressions in time domain for the closing speed and the LOS rotation rate.

Analysis in the arc-length system: Transforming the curvature command (9) to the arc-length system by using Eq. (3) and substituting the result into Eq. (8), we obtain

$$r\omega' + 2r'\omega = Nr'\omega \tag{11}$$

The closed-form solution of the LOS rotation rate is then obtained as [23]:

$$\omega = \omega_0 (r/r_0)^{N-2} \tag{12}$$

where ω_0 is the initial value of the LOS rotation rate. If $N > 2$, ω will decrease as r decreases and it will approach to zero at the end of the rendezvous. Thus, the first constraint mentioned previously is satisfied.

Analysis in the time domain: In classical differential geometry theory, the curvature $\kappa(s)$ represents the lateral acceleration, which is perpendicular to the velocity vector and changes the flight direction only. This acceleration is a normal component of the general acceleration composed of the control acceleration and gravitational acceleration. For the chaser and target in this paper, their normal acceleration magnitudes can be calculated as

$$a_m = V_m^2 \kappa_m, \quad a_t = V_t^2 \kappa_t \tag{13}$$

Transforming Eq. (8) to the time domain and combining with Eqs. (9) and (13), we obtain

$$a_{m\theta} = a_m (\boldsymbol{n}_m \cdot \boldsymbol{n}_{si}) = a_t (\boldsymbol{n}_t \cdot \boldsymbol{n}_{si}) - N\dot{r}\dot{\theta}_{si} \tag{14}$$

where $a_{m\theta}$ is used to control of the LOS rotation. Then, for a two-dimensional rendezvous problem, Eq. (13) can be rewritten as

$$a_{m\theta} = a_m \cos\theta_m = a_t \cos\theta_t - N\dot{r}\dot{\theta}_{si} \tag{15}$$

where θ_m and θ_t are respectively the angles between the LOS vector and the velocity vectors of the chaser and target.

The term $a_t \cos\theta_t$ in Eq. (15) is to compensate the target maneuvering in the normal direction of the LOS vector. Thus, the chaser can rendezvous with an arbitrarily maneuvering target, even if the target maneuver strategy is unpredictable. Consequently, the DG rendezvous algorithm performs as the augmented true proportional navigation (ATPN) guidance algorithm. For this reason, the DG rendezvous algorithm has the same performance as the ATPN guidance algorithm in the normal direction of the LOS vector.

Transforming Eq. (7) into the time domain and combining with Eq. (9), we obtain a time-varying second-order differential equation, as follows:

$$\ddot{r} = -Kr - D\dot{r} + d \tag{16}$$

where

$$K = \frac{V_t}{V_m} \left[\boldsymbol{t}_t \cdot \boldsymbol{t}_{si} - \frac{\boldsymbol{t}_t \cdot \boldsymbol{n}_{si}}{\boldsymbol{n}_m \cdot \boldsymbol{n}_{si}} (\boldsymbol{n}_m \cdot \boldsymbol{t}_{si}) \right] M_r$$

$$D = \frac{V_t}{V_m} \left[\boldsymbol{t}_t \cdot \boldsymbol{t}_{si} - \frac{\boldsymbol{t}_t \cdot \boldsymbol{n}_{si}}{\boldsymbol{n}_m \cdot \boldsymbol{n}_{si}} (\boldsymbol{n}_m \cdot \boldsymbol{t}_{si}) \right] M_v - N\dot{\theta}_{si} \frac{\boldsymbol{n}_m \cdot \boldsymbol{t}_{si}}{\boldsymbol{n}_m \cdot \boldsymbol{n}_{si}}$$

$$d = V_t^2 \left[\boldsymbol{n}_t \cdot \boldsymbol{t}_{si} - \frac{\boldsymbol{n}_t \cdot \boldsymbol{n}_{si}}{\boldsymbol{n}_m \cdot \boldsymbol{n}_{si}} (\boldsymbol{n}_m \cdot \boldsymbol{t}_{si}) \right] \kappa_t + r\dot{\theta}_{si}^2$$

The time-varying parameters K and D can be considered as the proportional and derivative gains of a PD-type controller and d can be considered as a time-varying external disturbance to a close-loop system. The relative range between the chaser and target r is then actively controlled, which means that the second constraint can also be guaranteed by selecting the three parameters N, M_r, and M_v properly. An equation similar to Eq. (16) can be found in Ref. [23], and a further study is needed to compare the two equations.

In summary, it has been shown that the two-dimensional DG rendezvous algorithm [23] controls the LOS rotation like an ATPN guidance algorithm in the normal direction of the LOS vector and it also controls the closing speed like a PD control law in the direction of the LOS vector.

3   ZEM/ZEV feedback guidance algorithm

In this section, the position vector of a chaser spacecraft is expressed simply as $\boldsymbol{r}$ without its subscript m for the purpose of notational simplicity.

3.1   Optimal control problem formulation

The orbital motion of a chaser spacecraft can be simply described in the ECI coordinate system as

$$\dot{\boldsymbol{r}} = \boldsymbol{V} \tag{17}$$

$$\dot{\boldsymbol{V}} = \boldsymbol{g}(\boldsymbol{r}) + \boldsymbol{a} \tag{18}$$

where $\boldsymbol{r}$ and $\boldsymbol{V}$ are respectively the position and velocity vectors of a chaser spacecraft; $\boldsymbol{a}$ is the control acceleration provided by the chaser's thrusters; $\boldsymbol{g}(\boldsymbol{r})$ represents the gravitational acceleration acting on the chaser that is generally a function of $\boldsymbol{r}$.

Given the initial time t_0 and the final terminal time t_f, the performance index J to be optimized is assumed as

$$J = \frac{1}{2} \int_{t_0}^{t_f} \boldsymbol{a}^{\mathrm{T}} \boldsymbol{a} \mathrm{d}t \tag{19}$$

This objective function is not to minimize the fuel consumption or ΔV directly. However, it provides a near-fuel-optimal characteristics for various practical examples [26–31].

The gravitational acceleration is, in general, a function of $\boldsymbol{r}$, which will not lead to an analytical solution of the optimal control problem. If the gravitational acceleration is assumed to be an explicit function of only time, the analytical optimal solution can be found [24,25]. The rendezvous problem can then be regarded as an optimization problem of determining the acceleration time history $\boldsymbol{a}(t)$ of the chaser subject to Eqs. (17) and (18) and a given set of initial and final conditions.

3.2   ZEM/ZEV feedback guidance algorithm for rendezvous

In order to find the analytical optimal solution, the final states (position and velocity vectors) of the target at t_f in the ECI coordinate system should be known in advance, which is different from the case of DG feedback guidance. Assuming that the target is moving in space subject to gravity only and that the final states can be predicted accurately, we have the given boundary conditions as

$$\boldsymbol{r}(t_0) = \boldsymbol{r}_0, \quad \boldsymbol{r}(t_f) = \boldsymbol{r}_f, \quad \boldsymbol{V}(t_0) = \boldsymbol{V}_0, \quad \boldsymbol{V}(t_f) = \boldsymbol{V}_f$$

The Hamiltonian function for this problem is defined as

$$H = \frac{1}{2} \boldsymbol{a}^{\mathrm{T}} \boldsymbol{a} + \boldsymbol{p}_r^{\mathrm{T}} \boldsymbol{V} + \boldsymbol{p}_v^{\mathrm{T}} (\boldsymbol{g}(t) + \boldsymbol{a}) \tag{20}$$

where $\boldsymbol{p}_r$ and $\boldsymbol{p}_v$ are the costate vectors associated with the position and velocity vectors, respectively. Notice that $\boldsymbol{g}$ is assumed as $\boldsymbol{g}(t)$ here.

The costate equations provide the optimal control solution expressed as a linear combination of the terminal values of the costate vectors $\boldsymbol{p}_r(t_f)$ and $\boldsymbol{p}_v(t_f)$. The optimal acceleration at any time t is then expressed as

$$\boldsymbol{a} = -t_{go} \boldsymbol{p}_r(t_f) - \boldsymbol{p}_v(t_f) \tag{21}$$

where $t_{go} = t_f - t$ is the time-to-go.

Solving the two-point boundary value problem in optimal control, we obtain the optimal control acceleration as

$$\boldsymbol{a} = \frac{6 \left[\boldsymbol{r}_f - \boldsymbol{r}(t_f) \right]}{t_{go}^2} - \frac{2 \left[\boldsymbol{v}_f - \boldsymbol{v}(t_f) \right]}{t_{go}} \tag{22}$$

where the term $\boldsymbol{r}_f - \boldsymbol{r}(t_f)$ denotes the difference between the specified final position and free-fall position at t_f, which is referred to as the ZEM distance; the term $\boldsymbol{v}_f -$

$v(t_f)$ denotes the difference between the specified final velocity and free-fall velocity at t_f, which is referred to as the ZEV error. If no additional control is commanded after the current time t, the final position and velocity vectors can be predicted as $r(t_f)$ and $v(t_f)$, which are referred to as the free-fall position and velocity vectors at t_f.

Finally, the ZEM/ZEV guidance algorithm for rendezvous can be expressed as

$$a = \frac{6}{t_{go}^2}\mathbf{ZEM} - \frac{2}{t_{go}}\mathbf{ZEV} \qquad (23)$$

where $\mathbf{ZEM} = r_f - r(t_f)$ and $\mathbf{ZEV} = v_f - v(t_f)$. To obtain the ZEM and ZEV terms, we need to calculate the free-fall position vector $r(t_f)$ and the velocity vector $v(t_f)$. As the simplest approach, these vectors can be predicted under the uniform gravity assumption. While this approach is only valid for short-range missions, its effectiveness is degraded for long-range missions in which the gravity direction change can not be ignored. In this case, the free-fall position and velocity vectors can be calculated by using Kepler's propagator or Vinti's propagator [30]. Then, we have the generalized ZEM/ZEV guidance of the form, Eq. (23), with the numerically propagated values of free-fall position and velocity vectors.

For an orbital rendezvous problem, a longer terminal time is known to be always better in minimizing the total control energy regardless of the initial conditions. This somewhat nontrivial problem is examined in Ref. [30] by generating the open-loop optimal solutions via general pseudo-spectral optimal control software (GPOPS) package. However, the ZEM/ZEV guidance algorithm wrongfully indicates a local optimal rendezvous time because the ZEM/ZEV performance rapidly deteriorates as the rendezvous time approaches the orbital period.

In this paper, we improve the long-range rendezvous ΔV performance of the ZEM/ZEV guidance by simply adding an initial drift phase as follows:

$$a = \begin{cases} \mathbf{0}_{3\times 1}, & t \leqslant t_1 \\ \frac{6}{t_{go}^2}\mathbf{ZEM} - \frac{2}{t_{go}}\mathbf{ZEV}, & t > t_1 \end{cases} \qquad (24)$$

where t_1 is a switching time to be properly selected such that $t_1 < t_f$. This is a simple version of the two-phase ZEM/ZEV guidance algorithm proposed in Ref. [31] for Mars and Lunar powered descent and landing problems

in an attempt to avoid a premature surface collision. The effectiveness of adding such a simple drift phase to the ZEM/ZEV guidance will be demonstrated in the next section. It is important to note that the switching time is determined by the initial positions of the chaser and target, as well as the orbital period. Unfortunately, no effort was made to explain how to select such a switching time for rendezvous problem. By investigating various initial conditions, we found that the local optimal rendezvous time of the ZEM/ZEV guidance is always a little larger than half orbital period. For instance, a standard circular orbit with 6000 s period approximately corresponds to a 3800 s local optimal rendezvous time, which is a natural outcome of the ZEM/ZEV algorithm. It should mention that, this conclusion only suits for a near-distance rendezvous mission, and the chaser and target initial orbits should be circular or near-circular.

4 Numerical simulation study results

4.1 An illustrative rendezvous example problem [23]

Numerical simulation study results of comparing the performance of the two distinct classes of feedback guidance algorithms are presented in this section. In this study, the position and velocity navigations are assumed to be isotropic in both the ECI and LVLH frame, and navigation errors, external disturbances, as well as orbital perturbations are ignored, which means that the final rendezvous position and velocity can be accurately predicted when the ZEV/ZEV algorithm is employed. Additionally, the Clohessy–Wiltshire–Hill coordinate system $(x,\ y,\ z)$ is used to describe the relative motion of the chaser with respect to the target. The origin of the CWH coordinates is located at the target, and x, y, z are along the radial, in-track, and cross-track directions, respectively.

In order to make the results more convincing and general, four chaser vehicles are chosen in this section, whose initial positions are located in the four quadrants of the CWH coordinate system, respectively. The orbital elements of the target and four chaser vehicles are listed together in Table 1, in which the eccentricity of each orbit is assumed as zero. When the range between the chaser and target vehicles becomes less than 3.0 m, computer simulation is stopped.

Table 1   Orbital elements of target and 4 chaser spacecraft [23]

	a (km)	e	i (deg)	Ω (deg)	ω (deg)	M_0 (deg)
Target	6840.2	0	98	35	0	0
Chaser 1	6871.0	0	98	35	0	0.6
Chaser 2	6871.0	0	98	35	0	−0.6
Chaser 3	6809.4	0	98	35	0	−0.6
Chaser 4	6809.4	0	98	35	0	0.6

4.2   Performance evaluation of DG rendezvous guidance

The DG rendezvous guidance was evaluated for various initial conditions and a wide range of terminal time, from which we found that the three guidance parameters N, M_r, and M_v are not independent. In other words, if two parameters are given, the third parameter should be properly tuned to satisfy a certain relationship between the three parameters. The study in Ref. [23] tried to optimize the whole rendezvous procedure and obtained convincing results; however, it made on attempt to establish the relationship between the three guidance parameters. In what follows, the relationship and effects of the three guidance parameters will be qualitatively given.

For Chaser 1, three cases ($M_r = 0.00000120$, 0.00000096,

and 0.00000070) are considered. As mentioned above, the control gain M_v needs to be adjusted with various M_r and N to make the closing speed converge to zero. Figures 2(a) and 2(b) show the variations of t_f and M_v versus N ranging from 2.1 to 3.7. The effect of N can be easily observed from these results, that is, both t_f and M_v will decrease as N gradually increases. Furthermore, we notice that the rendezvous time t_f cannot be arbitrarily selected for the DG guidance. It is indirectly selected by a combination of M_r and N, which is different from the ZEM/ZEV algorithm.

For Chaser 2, three cases ($N = 2.1$, 2.5, and 2.9) are further investigated, whose results are plotted in Figs. 2(c) and 2(d), respectively. As shown in Fig. 2(c), if we keep the same control gain M_r as a constant and apply a series of N ranging from 2.1 to 2.9, the range of the rendezvous window is less than 1200 s. However, if N is kept as 2.5, the rendezvous window is extended to 1800–6800 s by various M_r, which indicates that M_r has a greater impact on the rendezvous time than N for Chaser 2. Moreover, the effect of M_r also can be easily concluded from these results, that is, a smaller t_f and a lager M_v will be obtained under a larger M_r. With understanding the above discussion, the effects of M_r

(a) Corresponding t_f for Chaser 1 with various N (b) Corresponding M_v for Chaser 2 with various N

(c) Corresponding t_f for Chaser 2 with various M_r (d) Corresponding M_v for Chaser 2 with various M_r
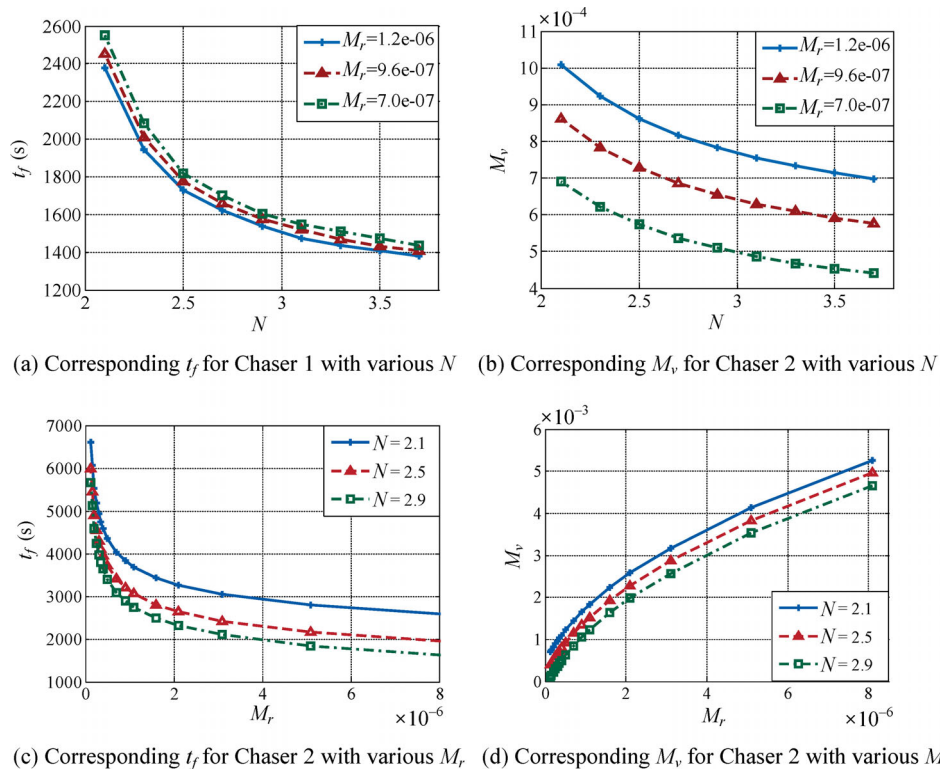
Fig. 2   Effects of the three design parameters of the DG rendezvous algorithm.

and N are clearly illustrated, and the third parameter M_v is natural outcome for various combination of M_r and N.

As shown in Fig. 2, if M_r is kept as 0.00000096, Chaser 2 will rendezvous with the target at 1776.2 s, 1587.8 s, and 1466.6 s when N is chosen as 2.5, 2.9, and 3.3, respectively. Figure 3 displays the detailed guidance performance of these three cases, including the relative motion trajectories, the closing speed magnitude, the acceleration command magnitude, and the ΔV requirement. Numerical simulation results demonstrate that the acceleration command a_m has some restriction and cannot increase arbitrarily. In the meanwhile, it can be observed from Fig. 3(c) that the peak of acceleration increases rapidly as the navigation ration increases, which should be avoided. In order to obtain an acceptable maximum acceleration, the navigation ratio N is capped at 3.7 for Chaser 1 in the previous discussion. Thus, there exists a proper rendezvous window, whose range is influenced by the three guidance parameters in the DG algorithm, subject to the relations shown in Fig. 2. This is a general conclusion appropriate for both the Chasers 1 and 2.

Figure 4 illustrates the overall rendezvous performance of the DG guidance for Chaser 2 with the rendezvous time is indirectly selected as 5981.3 s, 5446.6 s, and 4899.8 s, from which the similar conclusions can be inferred.

4.3 Performance evaluation of ZEM/ZEV guidance

To conduct a comparative evaluation, the rendezvous time considered for the DG guidance in the preceding section is also used as the specified terminal time of the ZEM/ZEV guidance in this section. It is worth mentioning that the rendezvous mission of Chaser 1 can be regarded as a short-range mission, because the rendezvous time is much less than the orbital period of about 6000 s. Consequently, a conventional, single-phase ZEM/ZEV can be employed and compared with the DG guidance.

Figure 5 displays the guidance performance of the conventional, single-phase ZEM/ZEV algorithm for Chaser 1, including the relative motion trajectories, the closing speed magnitude, the acceleration command magnitude, and the ΔV requirement. Comparing Figs. 3 and 5, we can notice that the maximum control acceleration of the ZEM/ZEV guidance is smaller than that of the DG guidance for Chaser 1. However, the DG guidance requires a smaller terminal acceleration
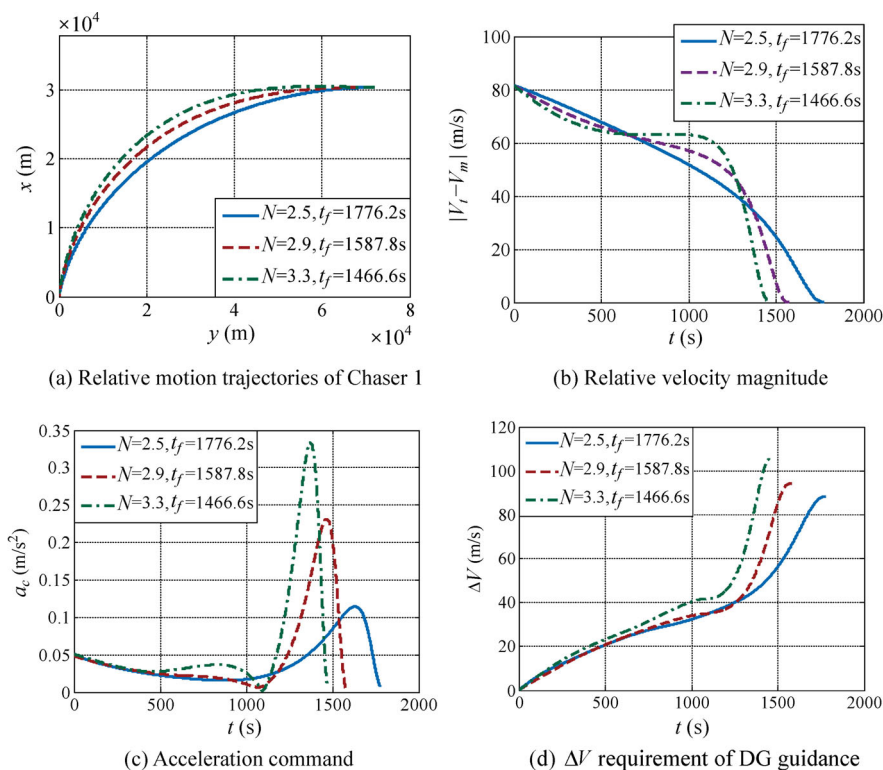

(a) Relative motion trajectories of Chaser 1

(b) Relative velocity magnitude

(c) Acceleration command

(d) ΔV requirement of DG guidance

Fig. 3 DG guidance performance for Chaser 1.

(a) Relative motion trajectories of Chaser 2

(b) Relative velocity magnitude

(c) Acceleration command

(d) ΔV requirement of DG guidance

Fig. 4 DG guidance performance for Chaser 2.

(a) Relative motion trajectories of Chaser 1

(b) Relative velocity magnitude
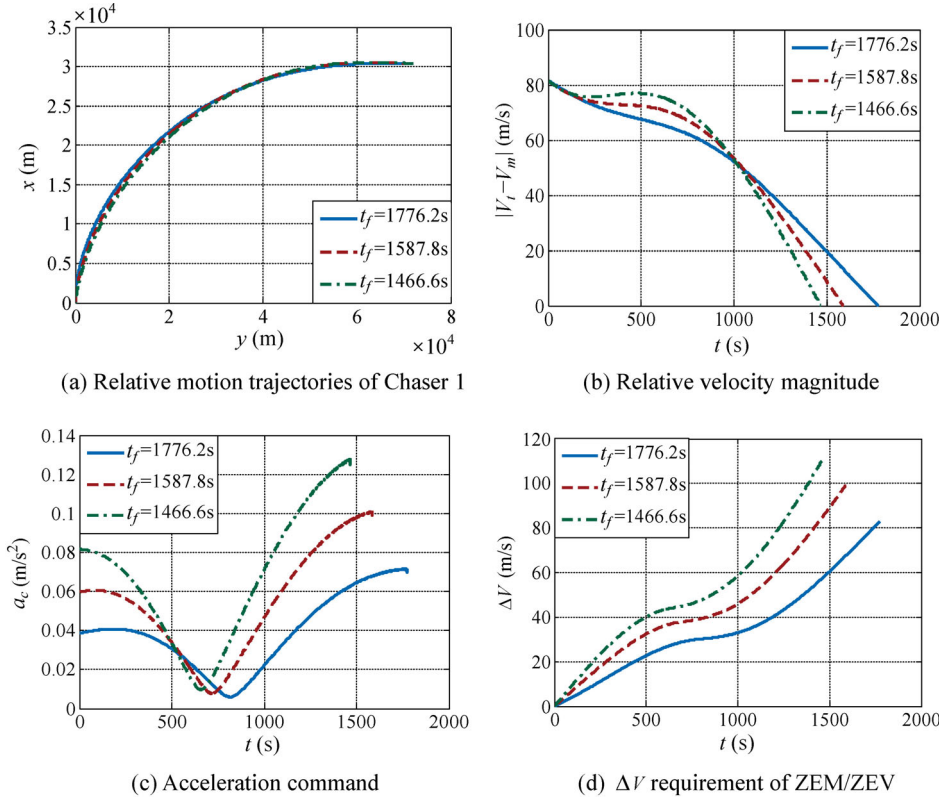
(c) Acceleration command

(d) ΔV requirement of ZEM/ZEV
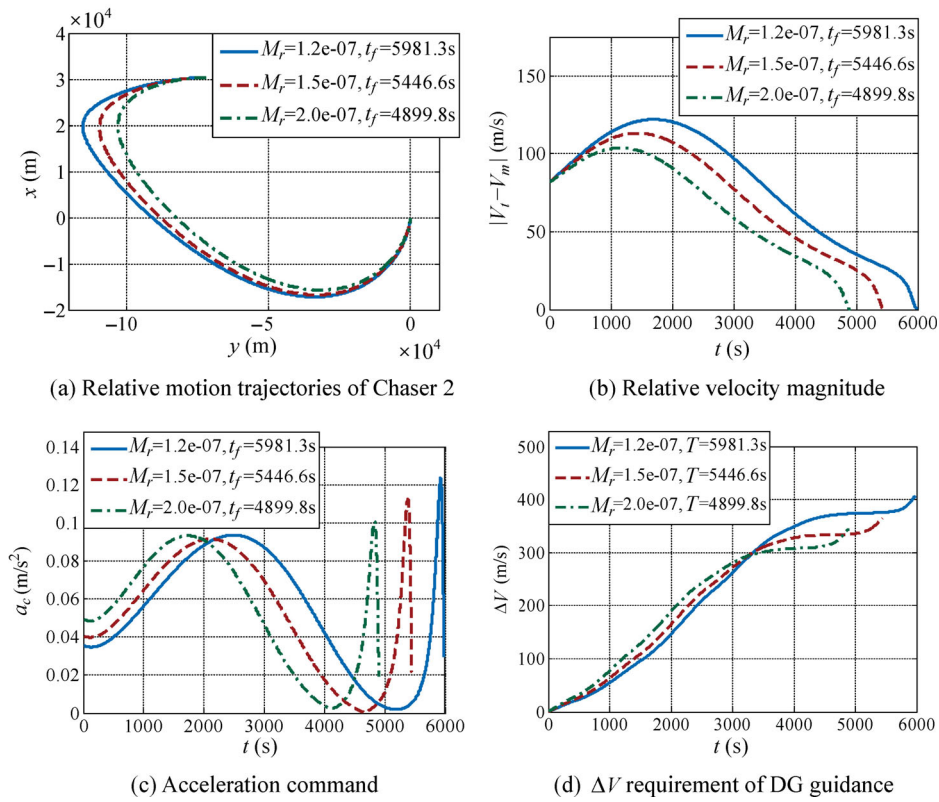
Fig. 5 Single-phase ZEM/ZEV guidance performance for Chaser 1.

because the LOS rotation rate will decrease to zero at the end of rendezvous.

As was discussed for the DG guidance, the rendezvous time of Chaser 2, considered by the DG guidance, is much longer than that of Chaser 1, even approaching the orbital period of about 6000 s. Therefore, the rendezvous mission for Chaser 2 is considered as a long-range mission, in which the two-phase ZEM/ZEV guidance concept [30] may need to be employed. Figure 6 illustrates the performance of the two-phase ZEM/ZEV guidance with a given 5446.6 s rendezvous time and three different values of switching time t_1 (1000 s, 1500 s, and 2000 s, which keeps the actual rendezvous time being a little larger than half orbital period).

We notice that the smallest ΔV is about 232.2 m/s when t_1 is chosen as 1000 s. We also notice that the relative position along the x-axis is naturally kept at the initial altitude of 31 km during the drift phase, while the y-axis position drift freely. Furthermore, the maximum acceleration of the ZEM/ZEV guidance is larger than that of the DG guidance, which is different from the case of Chaser 1.

To provide a further detailed comparison, we consider four chaser vehicles as described in Table 1.
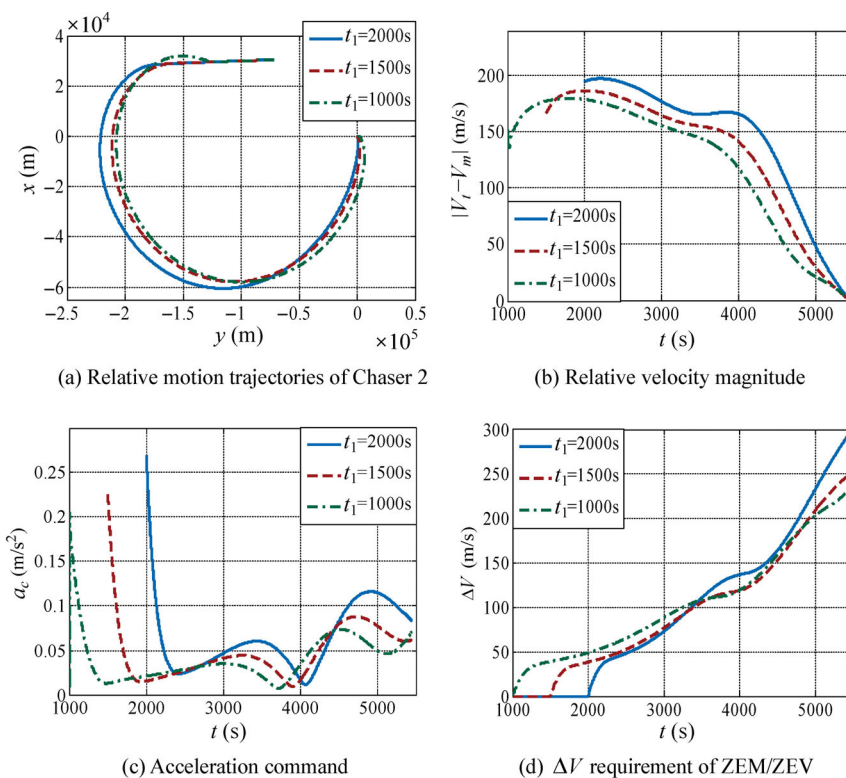
Their relative motion trajectories are provided in Fig. 7. These trajectories depict some well-known characteristics of the relative motion in the CWH coordinate system. We also see that the rendezvous with the initial conditions in the second and fourth quadrants require more time than those in the first and third quadrants. Hence, by using the DG and ZEV/ZEV guidance, we think the first and third quadrants are the proper initial relative position for rendezvous missions.

4.4 Performance comparison of DG guidance, ZEM/ZEV guidance, and open-loop optimization

The ΔV performance of the two guidance algorithms is compared with the open-loop optimal solutions to further evaluate their orbital rendezvous performance. General pseudospectral optimal control software (GPOPS) is a versatile open-source multiphase optimizer and is used in this paper to generate the open-loop optimal solutions.

Figure 8(a) provides the ΔV performance of the DG guidance for Chaser 1 with various values of M_r. We notice that the ΔV performance of the DG guidance is affected by the rendezvous time as well as the control gain M_r. However, no matter what the value of M_r
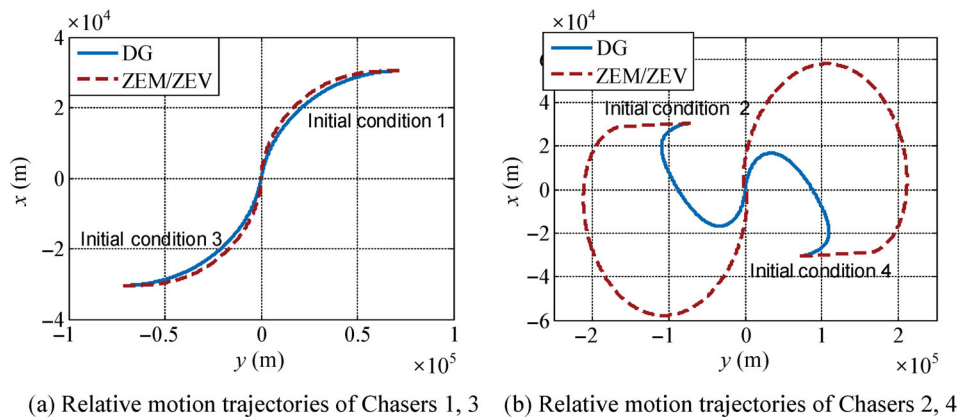

(a) Relative motion trajectories of Chaser 2

(b) Relative velocity magnitude

(c) Acceleration command

(d) ΔV requirement of ZEM/ZEV

Fig. 6   Two-phase ZEM/ZEV guidance performance for Chaser 2.

(a) Relative motion trajectories of Chasers 1, 3   (b) Relative motion trajectories of Chasers 2, 4

Fig. 7   Comparison of relative motion trajectories for DG and ZEM/ZEV guidance.

is, the ΔV decreases as the rendezvous time increases. Figure 8(b) provides the ΔV performance of the DG (M_r is 0.00000120) and ZEM/ZEV guidance, in comparison with the open-loop optimization solutions for Chaser 1. The ZEM/ZEV algorithm can even compete with the corresponding open-loop optimal solutions for the short-range rendezvous mission. Although the ZEM/ZEV is a near-fuel-optimal approach, its ΔV is not always better than the DG guidance. Especially, the ΔV of the DG guidance is 6.4% less than that of the ZEM/ZEV when the rendezvous time is required as 1641.2 s.

So far, the ΔV performance of the DG guidance with various parameters has been clearly illustrated by Fig. 8(a). Now, the performance of the two-phase ZEM/ZEV algorithm presented in Eq. (24) for a long-range mission should be further investigated. Figure 8(c) gives the ΔV plots of the two-phase ZEM/ZEV guidance for Chaser 2, in which the ΔV performance needs to be improved, especially compared with the single-phase ZEM/ZEV guidance of Chaser 1. As can be noticed in Fig. 8(c), the ZEM/ZEV guidance, with an initial drift phase with no control, has ability to decrease
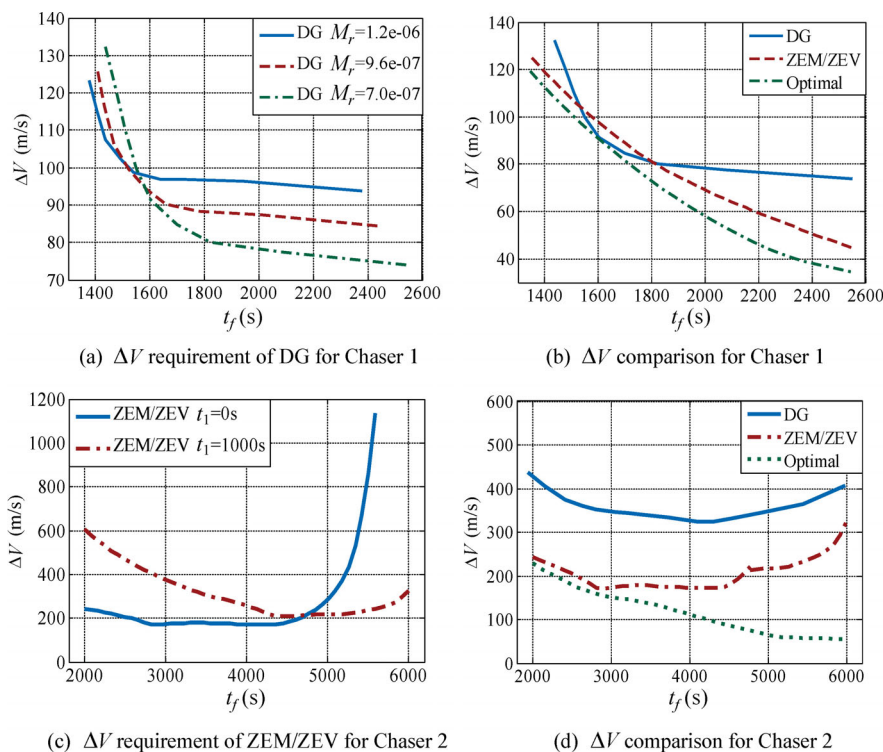

(a) ΔV requirement of DG for Chaser 1   (b) ΔV comparison for Chaser 1

(c) ΔV requirement of ZEM/ZEV for Chaser 2   (d) ΔV comparison for Chaser 2

Fig. 8 ΔV performance comparison of DG, ZEM/ZEV (with drift phase), and open-loop optimization.

the actual fuel consumption for a long-range, slower rendezvous. According to the comparative results, when t_1 is chosen as 1000 s, the local optimal rendezvous time of the two-phase ZEM/ZEV is about 4400 s, which is longer than the optimal time indicated by the single-phase ZEM/ZEV (about 2800 s). Thus, the two-phase ZEM/ZEV guidance wrongfully indicates a local optimal rendezvous time as well, which is determined by the ZEM and ZEV terms. However, the local optimal rendezvous time can be properly extended to adjust to a long-range rendezvous mission by using the two-phase ZEM/ZEV guidance.

Figure 8(d) provides the performance comparison of the DG ($N = 2.5$), the ZEM/ZEV (t_1=1000 s), and the open-loop optimization solutions for Chaser 2. The ΔV of the DG guidance also has a local optimal value of ΔV, in which the rendezvous time is about 4100 s. It is worth mentioning that, the optimal rendezvous time of the DG guidance depends on N.

In summary, the DG guidance is not designed to optimize the fuel consumption or control energy, and its ΔV performance is natural outcome of the initial conditions and guidance parameters. Compared with the open-loop optimal solutions, the DG guidance always requires a larger ΔV, but sometimes its requirement is acceptable, such as the Chaser 1 shown in Fig. 8(b). The ZEM/ZEV guidance focused on the control energy optimization, epically for a short-range rendezvous, in which its ΔV performance can even compete with the open-loop optimal solutions. The proposed two-phase ZEM/ZEV algorithm (24) can effectively decrease ΔV requirement for a long-range rendezvous, which is a meaningful extension of the two-phase concept presented in Ref. [31]. After remedying, we have to say that the ΔV performance for long-range rendezvous missions is still not near-optimal, but improved a lot.

Based on the numerical study results as described in this paper, an overall performance assessment of the DG and ZEM/ZEV guidance is provided in Table 2.

Table 2 Comparison of the DG and ZEM/ZEV guidance algorithms

	DG	ZEM/ZEV
Rendezvous time	no direct control	can be directly specified
Terminal states	open	to be specified
Target trajectory info	required	not required
Implementation	complex	simple
ΔV requirement	always larger than optimal	depends on the rendezvous range

5   Conclusions

The ΔV performance of two distinct classes of feedback guidance algorithms has been compared for a rendezvous maneuver utilizing continuous low-thrust engines, with various initial conditions and a wide range of terminal time of less than one orbital period. Each of the DG (Differential Geometric) and ZEM/ZEV (Zero-Effort-Miss/Zero-Effort-Velocity) feedback guidance algorithms has been shown to possess its unique pros and cons over each other. The ZEM/ZEV feedback guidance algorithm and its appropriate variants have been shown to be a practical solution to a non-impulsive rendezvous problem because of its simplicity and overall satisfactory ΔV performance. However, a further study is needed to combine the classical impulsive ΔV techniques with the continuous DG and ZEM/ZEV feedback guidance algorithms for a multiple-revolution rendezvous problem.

Acknowledgements

References

[1]   Goodman, J. L. History of space shuttle rendezvous and proximity operations. *Journal of Spacecraft and Rockets*, **2006**, 43(5): 944–959.

[2]   Barbee, B., Carpenter, J. R., Heatwole, S., Markley, F. L., Moreau, M., Naasz, B. J., Van Eepoel, J. A guidance and navigation strategy for rendezvous and proximity operations with a noncooperative spacecraft in geosynchronous orbit. *The Journal of the Astronautical Sciences*, **2011**, 58(3): 389–408.

[3]   Wen, C., Gurfil, P. Guidance, navigation and control for autonomous R-bar proximity operations for geostationary satellites. *Proceedings of the Institution of Mechanical Engineers, Part G: Journal of Aerospace Engineering*, **2017**, 231(3): 452–473.

[4]   Luo, Y.-Z., Sun, Z.-J. Safe rendezvous scenario design for geostationary satellites with collocation constraints. *Astrodynamics*, **2017**, 1(1): 71–83.

[5]   Zhang, S., Han, C., Sun, X. New solution for rendezvous between geosynchronous satellites using low thrust. *Journal of Guidance, Control, and Dynamics*, **2018**, 41(6): 1396–1405.

[6] Wang, W., Chen, L., Li, K., Lei, Y. One active debris removal control system design and error analysis. *Acta Astronautica*, **2016**, 128: 499–512.

[7] Wang, W., Song, X., Li, K., Chen, L. A novel guidance scheme for close range operation in active debris removal. *Journal of Space Safety Engineering*, **2018**, 5(1): 22–33.

[8] Chiou, Y.-C., Kuo, C.-Y. Geometric approach to three-dimensional missile guidance problem. *Journal of Guidance, Control, and Dynamics*, **1998**, 21(2): 335–341.

[9] Kuo, C.-Y., Chlou, Y.-C. Geometric analysis of missile guidance command. *IEEE Proceedings: Control Theory and Applications*, **2000**, 147(2): 205–211.

[10] Kuo, C.-Y., Soetanto, D., Chiou, Y.-C. Geometric analysis of flight control command for tactical missile guidance. *IEEE Transactions on Control Systems Technology*, **2001**, 9(2): 234–243.

[11] Li, C., Jing, W., Wang, H., Qi, Z. iterative solution to differential geometric guidance problem. *Aircraft Engineering and Aerospace Technology*, **2006**, 78(5): 415–425.

[12] Li, C., Jing, W. Analysis of 3D geometric guidance problem. *Transactions of the Japan Society for Aeronautical and Space Sciences*, **2008**, 51(172): 124–129.

[13] Li, C., Jing, W., Qi, Z., Wang, H. A novel approach to the 2D differential geometric guidance problem. *Transactions of the Japan Society for Aeronautical and Space Sciences*, **2007**, 50(167): 34–40.

[14] Li, C.-Y., Jing, W.-X. Fuzzy PID controller for 2D differential geometric guidance and control problem. *IET Control Theory & Applications*, **2007**, 1(3): 564–571.

[15] Li, C., Jing, W., Wang, H., Qi, Z. Gain-varying guidance algorithm using differential geometric guidance command. *IEEE Transactions on Aerospace and Electronic Systems*, **2010**, 46(2): 725–736.

[16] Dhananjay, N., Ghose, D., Bhat, M. S. Capturability of a geometric gudiance law in relative velocity space. *IEEE Transactions on Control Systems Technology*, **2009**, 17(1): 111–122.

[17] Li, K., Chen, L., Bai, X. Differential geometric modeling of guidance problem for interceptors. *Science China Technological Sciences*, **2011**, 54(9): 2283–2295.

[18] Li, K., Chen, L., Tang, G. Improved differential geometric guidance commands for endoatmospheric interception of high-speed targets. *Science China Technological Sciences*, **2013**, 56(2): 518–528.

[19] Li, K., Chen, L., Tang, G. Algebraic solution of differential geometric guidance command and time delay control. *Science China Technological Sciences*, **2015**, 58(3): 565–573.

[20] Li, K., Su, W., Chen, L. Performance analysis of three-dimensional differential geometric guidance law against low-speed maneuvering targets. *Astrodynamics*, **2018**, 2(3): 233–247.

[21] Ariff, O., Zbikowski, R., Tsourdos, A., White, B. A. Differential geometric guidance based on the involute of the target's trajectory. *Journal of Guidance, Control, and Dynamics*, **2005**, 28(5): 990–996.

[22] White, B. A., Zbikowski, R., Tsourdos, A. Direct intercept guidance using differential geometric concepts. *IEEE Transactions on Aerospace and Electronic Systems*, **2007**, 43(3): 899–919.

[23] Meng, Y., Chen, Q., Ni, Q. A new geometric guidance approach to spacecraft near-distance rendezvous problem. *Acta Astronautica*, **2016**, 129: 374–383.

[24] Ebrahimi, B., Bahrami, M., Roshanian, J. Optimal sliding-mode guidance with terminal velocity constraint for fixed-interval propulsive maneuvers. *Acta Astronautica*, **2008**, 62(10–11): 556–562.

[25] Furfaro, R., Selnick, S., Cupples, M. Nonlinear sliding guidance algorithms for precision lunar landing. In: Proceedings of the 21st AAS/AIAA Space Flight Mechanics Meeting, **2011**: AAS 2011-167.

[26] Guo, Y., Hawkins, M., Wie, B. Optimal feedback guidance algorithms for planetary landing and asteroid intercept. In: Proceedings of the AAS/AIAA Astrodynamics Specialist Conference, **2011**: AAS 2011-588.

[27] Guo, Y., Hawkins, M., Wie, B. Applications of generalized zero-effort-miss/zero-effort-velocity feedback guidance algorithm. *Journal of Guidance, Control, and Dynamics*, **2013**, 36(3): 810–820.

[28] Guo, Y., Hawkins, M., Wie, B. Waypoint-optimized zero-effort-miss/zero-effort-velocity feedback guidance for Mars landing. *Journal of Guidance, Control, and Dynamics*, **2013**, 36(3): 799–809.

[29] Ahn, J., Guo, Y., Wie, B. Precision ZEM/ZEV feedback guidance algorithm utilizing Vinti's analytic solution of perturbed Kepler problem. In: Proceedings of the AAS/AIAA Space Flight Mechanics Meeting, **2016**: AAS 16-345.

[30] Ahn, J., Wang, P., Guo, Y., Wie, B. Optimal terminal-time determination for the ZEM/ZEV feedback guidance law. *Astrodynamics*, **2019**. (to be published)

[31] Wie, B. Two-phase ZEM/ZEV guidance for Mars and Lunar powered descent & landing with hazard avoidance and retargeting. Keynote Talk in the 4th IAA Conference on Dynamics and Control of Space Systems, **2018.**

[32] Wie, B., Zimmerman, B., Lyzhoft, J., Vardaxis, G. Planetary defense mission concepts for disruptiong/ pulverizing harzadous asteroids with short wanrning time. *Astrodynamics*, **2017**, 1(1): 3–21.

Yanning Guo received his Ph.D. degree in control science and engineering from Harbin Institute of Technology, China, in 2012, and was a visiting scholar at Iowa State University in 2010–2011. Currently, he is an associate professor at Harbin Institute of Technology, and specializes in optimal control, sliding-mode control, as well as visual navigation and localization.

Pengyu Wang received his B.S. degree in automation from Harbin Engineering University, China, in 2015, and M.S. degree in control science and engineering from Harbin Institute of Technology, China, in 2017. He is now a Ph.D. candidate at Harbin Institute of Technology focusing on the development and application of control theories in aerospace problems, including Mars pinpoint landing, spacecraft rendezvous, and missile impact-time guidance, etc. E-mail: wangpy_hit@163.com.

Bong Wie is a professor of aerospace engineering at Iowa State University. He is the founding director of the Asteroid Deflection Research Center established in 2008 at Iowa State University. He received his M.S. and Ph.D. degrees in aeronautics and astronautics from Stanford University in 1978 and 1981, respectively. In 2006, the AIAA (American Institute of Aeronautics and Astronautics) presented Prof. Wie with the Mechanics and Control of Flight Award for his innovative research on advanced control of complex spacecraft such as agile imaging satellites, solar sails, and large space structures. E-mail: bongwie@iastate.edu.